

Asymmetric Mathieu beams

Arturo Barcelo-Chong (白文雄), Brian Estrada-Portillo, Arturo Canales-Benavides,
and Servando Lopez-Aguayo*

Tecnologico de Monterrey, Escuela de Ingeniería y Ciencias, Monterrey 64849, México

*Corresponding author: servando@itesm.mx

Received September 3, 2018; accepted October 22, 2018; posted online November 27, 2018

We report the generation of asymmetric Mathieu beams: invariant intensity optical profiles that can be described by three parameters. The first one describes the amount of ellipticity, the second one takes into account the degree of asymmetry of the profile, and the third parameter denotes the angular position, where it is localized with the respective asymmetry. We propose a simple angular spectrum to generate these nondiffracting beams, and we report how it changes their distribution of power and orbital angular momentum in function with their ellipticity and degree of asymmetry. We confirm the existence of these invariant beams by propagation in an experimental setup.

OCIS codes: 260.1960, 140.3300, 070.3185.

doi: 10.3788/COL201816.122601.

Optical lattices are artificial structures of light generated by interfering optical laser beams, which creates a standing wave pattern that induces a spatially dependent potential energy that can be useful for the study and applications of light-matter interactions^[1]. Optical lattices have been used for the detection of single atoms by a quantum gas microscope^[2] in the study of parity-time symmetry periodic potentials^[3], in the generation of quantum logic gates^[4], and for soliton routing^[5] among other applications. In particular, a possibility to generate these optical landscapes is by interfering several controlled beams^[6], where nondiffracting beams (NBs) are ideal candidates due to their only change in phase during propagation. The NBs are particular solutions to the Helmholtz equation given by

$$(\nabla^2 + k^2)E(x, y, z) = 0, \quad (1)$$

where $k = 2\pi/\lambda$ is the wave number of a monochromatic scalar light field E with a wavelength of λ . It is known, as a result from group theory^[7], that the Helmholtz equation is separable in eleven coordinate systems, but there are only four coordinate systems that allow solutions that preserve the same intensity profile of their transverse optical field, yielding only phase changed solutions along the propagation axis: the Cartesian, the circular, the elliptical, and the parabolic cylindrical coordinate systems. For each one of these particular coordinate systems, it is possible to obtain as natural invariant beams the plane waves, Bessel beams^[8,9], Mathieu beams^[10], and parabolic beams^[11], respectively. An alternative description of the NBs can be done via the Whittaker integral^[9,12],

$$E(x, y, z) = F \int_0^{2\pi} A(\phi) \exp[ik_t(x \cos \phi + y \sin \phi)] d\phi, \quad (2)$$

where ϕ represents the azimuthal angle in the frequency space, while $A(\phi)$ is the angular spectrum of the beam.

The transverse k_t and longitudinal k_z components of the k wave vector satisfy the expression $k^2 = k_z^2 + k_t^2$. Variable z stands for the spatial longitudinal coordinate, while x and y stand for spatial transverse coordinates. The function $F = \exp(ik_z z)$ is just a phase z -dependent term that does not contribute to modifying the intensity of the NB in propagation. It is important to remark that the angular spectrum for the case of an NB is only defined on an infinitely narrow ring of radius k_t .

In this Letter, by solving Eq. (2), we report the generation of invariant asymmetric Mathieu (AM) beams, which can be considered as a kind of generalization of the asymmetric Bessel beams introduced in the seminal works by Kotlyar *et al.*^[13]. We demonstrate an alternative approach to generate a kind of asymmetric beam by directly using Eq. (2), we calculate the respective variation of power and orbital angular momentum (OAM) in a function of their ellipticity and asymmetry parameters, and finally, we demonstrate that these beams can indeed be generated into an experimental setup. Since the pioneering work on nondiffracting Bessel beams due to Durnin^[8,9], there has been an intense study of novel NBs and potential applications oriented towards nonlinear optics, imaging, and micromanipulation, among many other areas^[14]. Besides the four families of NBs previously mentioned, there are even more complex nondiffracting structures, such as Lommel modes^[15] and half-Pearcey beams^[16]. In fact, it is possible to build complex optical lattices on demand by using relaxation procedures^[12] or genetic algorithms^[17]. Nowadays, Mathieu beams have been also used in the study of laser micromachining^[18], parity-time systems^[19], and for the control of optical solitons in photonic lattices^[20]. Generating Mathieu beams involves the following coordinates transformation to Eq. (1): $x = h \cosh \xi \cos \eta$, $y = h \sinh \xi \sin \eta$, and, taking into account the limits of both η , the angular, and ξ , the radial variables, which are $[0, 2\pi)$ and $[0, \infty)$, respectively. Parameter $2h$ stands for the interfocal separation. The

solutions result from solving Eq. (1) in the form of $E = \Theta(\eta)R(\xi)\exp(ik_z z)$, where $\Theta(\eta)$ and $R(\xi)$ solve the angular and radial Mathieu equations, respectively, given by

$$\left[\frac{d^2}{d\eta^2} + (a - 2q \cos 2\eta) \right] \Theta(\eta) = 0, \quad (3)$$

$$\left[\frac{d^2}{d\xi^2} - (a - 2q \cosh 2\xi) \right] R(\xi) = 0, \quad (4)$$

where the ellipticity parameter is given by $q = h^2 k_t^2 / 4$, and a is a separation constant that results from the variable separation method. In fact, given a q value, there are countably several special values of a , called characteristic values, where the Mathieu equations admit solutions with periodic behavior of either 2π or π . In particular, when the eigenvalues a belong to a discrete set, the solutions are of an integral order, otherwise they are of a fractional order.

These kinds of solutions are of special physical interest due to the continuity condition at $\Theta(\eta = 0) = \Theta(\eta = 2\pi)$. Therefore, an even Mathieu beam can be represented as

$$E_e(\xi, \eta, z) = C e_n(\xi, q) c e_n(\eta, q) \exp(ik_z z), \quad (5)$$

where $C e_n(\xi, q)$ and $c e_n(\eta, q)$ stand for the n th order of the even radial Mathieu function and the even angular Mathieu function of the first kind, respectively. Similarly, the odd Mathieu beams can be represented by

$$E_o(\xi, \eta, z) = S e_n(\xi, q) s e_n(\eta, q) \exp(ik_z z), \quad (6)$$

where $S e_n(\xi, q)$ and $s e_n(\eta, q)$ represent the n th-order odd radial Mathieu function and the odd Mathieu function of the first kind, respectively. Note that even though Mathieu beams do not carry OAM by themselves, the linear combination between even and odd Mathieu beams with complex amplitudes do carry OAM. It is important to remark that any idealized NB demands infinite energy due to its infinite extension. However, it has been demonstrated that NB can be apodized by a well-localized function, such as a Gaussian one, and then the resulting finite energy beam still displays invariant behavior for a finite distance of propagation, as is the case of the Helmholtz–Gauss waves in general^[21] and the physical version of asymmetric Bessel modes, the asymmetric Bessel–Gauss beams^[22]. The corresponding angular spectrum of these physically realizable finite NBs then becomes an annular ring with width $4/\omega_0$, where ω_0 is a parameter related to the Gaussian width.

Next, in order to introduce the AM beams, we propose a modification over the angular variable ϕ in Eq. (2). We set a new azimuth angle variable in the frequency space ϕ' by using the following transformation

$$\phi' = \phi + i\alpha \cos(\phi + \beta), \quad (7)$$

where $\alpha \in [0, \infty)$ determines the asymmetry degree of the profile, and $\beta \in [0, 2\pi)$ is a rotation parameter that determines the part in which the quasi-ring is going to be located at the breaking point of asymmetry. In the following, we omit primes for simplicity. Next, we generate the corresponding AM beams by using an angular spectrum,

$$A(\phi) = c e_m(\phi, q) \pm i s e_m(\phi, q), \quad (8)$$

where $c e_m(\phi, q)$ and $s e_m(\phi, q)$ stand for the even and odd angular Mathieu function of the first kind of order m , respectively. Finally, in order to recover the corresponding complex profile of the optical field, we computationally solve Eq. (2).

In Fig. 1, we show the profiles generated by the proposed technique. Without loss of generality, here we report a fourth-order AM beam with $q = 1$, and a third-order AM beam with $q = 2$. Note that higher q values physically generate a higher degree of ellipticity in the shape of the beam, while it is possible to set the location of the maximum intensity value by only modifying the β parameter in the respective angular spectrum. Thus, using Eq. (7), we can control either ellipticity and angular localization of asymmetry of these Mathieu beams. By setting $\alpha = 0$, note that we recover the standard and elliptically symmetric Mathieu beams. In a similar fashion, the modification of q , α , and β parameters, which stand for change in ellipticity, asymmetry, and localization of the

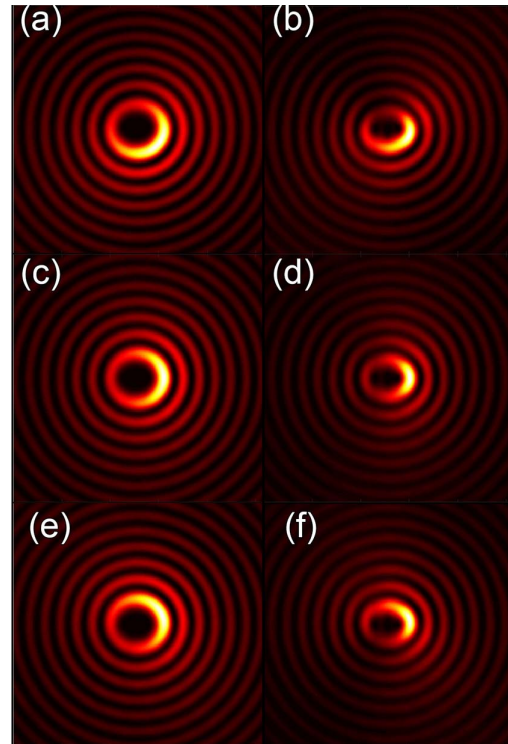


Fig. 1. Intensity of AM beams for the case of a fourth-order $q = 1$ and angular phase shift β parameters of (a) $\pi/4$, (c) $\pi/2$, and (e) $2\pi/3$. A third-order AM beam with $q = 2$ and β parameters of (b) $\pi/4$, (d) $\pi/2$, and (f) $2\pi/3$.

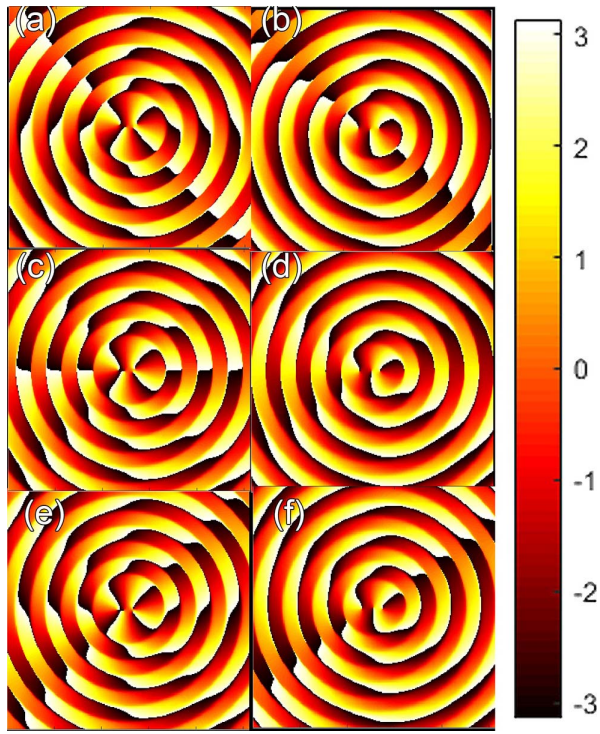


Fig. 2. Phase distribution of AM beams, where (a), (c), and (e) are fourth order with ellipticity parameter $q = 1$ and angular phase shift given by β parameters of $\pi/4$, $\pi/2$, and $2\pi/3$, respectively. (b), (d), and (f) correspond to third-order AM beams with $q = 2$ and β parameters of $\pi/4$, $\pi/2$, and $2\pi/3$, respectively.

maximum, respectively, has an impact in the phase distribution of the profile, as is shown in Fig. 2. Note that for the fourth-order case, there are four optical singularities, whose corresponding phase distribution and location are modified in function of the β parameter. Similar behavior is observed for the third-order case. These elliptic vortices can be used for rotating microscopic particles^[23]. The proposed variable transformation given by Eq. (7) allows a rich variety of possible asymmetric NBs, as shown in Fig. 3, where we set $\beta = 0$ and focus to change either q or α parameters. Note that with $q = 0$ we recover the Bessel modes, and by modifying the q parameter, we can mimic the Bessel asymmetric modes previously reported in the influential works of Kotlyar *et al.*^[13,22].

By using the method proposed here, we are able to generate asymmetric Bessel beams, where the rings show a small asymmetry, or half-Bessel-like beam, where an angular sector has a null intensity, similar to the tight focusing of an asymmetric Bessel beam^[24]; or, we can even shape profiles with more continuous distribution of light, resembling the quasi-one-dimensional optical lattices reported in Ref. [25].

By modifying the q parameter, note that the circular symmetry is broken, and we observe an elliptical shape that is similar for the circular case, and we can control the degree of symmetry by changing the α parameter. If we increase even more the parameter q , the continuity along the intensity is also broken, and it is also easier

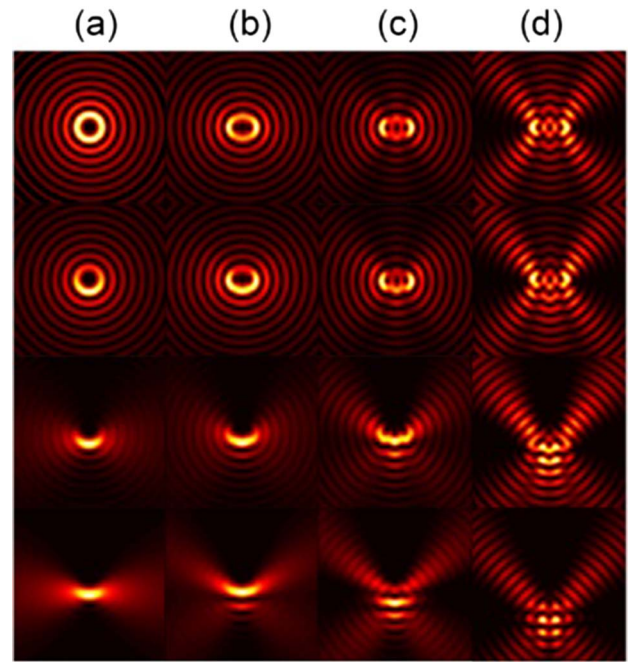


Fig. 3. Intensity of AM beams. (a) $q = 0.01$, (b) $q = 2$, (c) $q = 5$, and (d) $q = 15$. In all cases, from top to bottom, $\alpha = 0$, $\alpha = 0.1$, $\alpha = 0.5$, and $\alpha = 1$.

to see the localization of the corresponding elliptical vortices. Finally, further increase of the q parameter moves toward more exotic shapes. In fact, the elliptical cylindrical coordinates degenerate into the Cartesian cylindrical coordinates as $q \rightarrow \infty$, while for $q \rightarrow 0$, we recover the circular cylindrical coordinate system.

As a next step, we generate the corresponding physically realizable AM beams. Hence, we simply use the corresponding nondiffracting patterns discussed previously but now apodized by a Gaussian function, and thus, we obtain the corresponding Helmholtz–Gauss version of the AM beams. We show some profiles in Fig. 4. As the corresponding number of rings is faded by the corresponding Gaussian envelope, the width of the corresponding angular spectrum is also increased, as is expected^[12]; however, note that the topology of the AM beams remains similar to their nondiffracting counterpart, only being diminished in the amplitude that is naturally done by the localized apodization. Thus, we report that the shape of the beams introduced here can indeed be realizable in an experimental setup, as is shown in Fig. 5.

In order to demonstrate the complete feasibility of these AM beams, we use a transmissive spatial light modulator with a resolution of 600 pixel \times 800 pixel. First, an image of the modulated pattern is sent to the spatial light modulator, which is then illuminated using a collimated plane wave generated by a He–Ne laser. It is possible to obtain the angular spectrum of the modulated pattern at the back focal plane of a positive lens of 500 mm focal length, where an iris diaphragm is used to filter out all of the high diffraction orders. The iris diaphragm is at the frontal focal plane of a second lens of 300 mm focal length, which

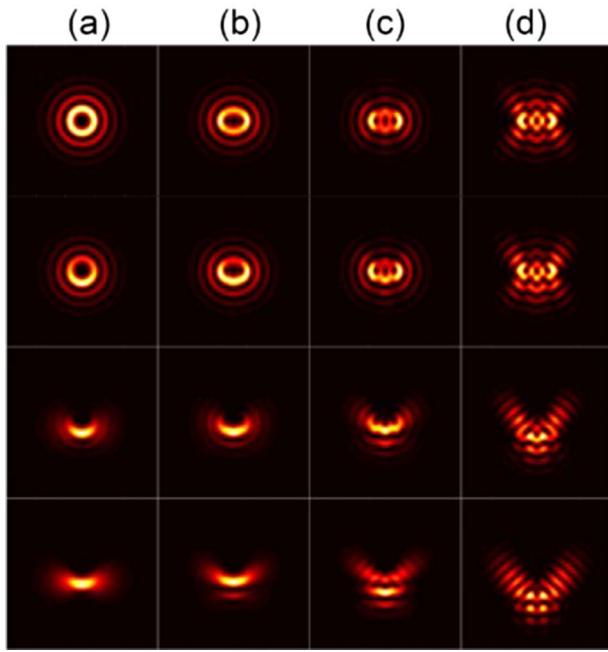


Fig. 4. Intensity of asymmetric Gaussian–Mathieu beams with the following parameters: (a) $q = 0.01$, (b) $q = 2$, (c) $q = 5$, and (d) $q = 15$. In all cases, from top to bottom, $\alpha = 0$, $\alpha = 0.1$, $\alpha = 0.5$, and $\alpha = 1$.

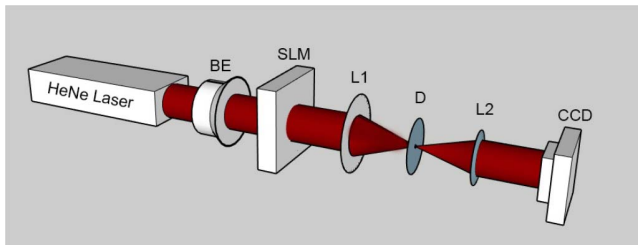


Fig. 5. Experimental setup. From left to right: He–Ne laser at 633 nm, 12 mW; BE, beam expander, 10 \times ; SLM, spatial light modulator, LC2002; L1 and L2, lenses; D, diaphragm; CCD, Thorlabs CCD.

finally allows the generation of the required invariant field. The diverse intensity profiles of the AM beams were recorded by using a CCD with 1280 pixel \times 1024 pixel at several planes along the corresponding axis of the evolution of 20 cm, where the corresponding Rayleigh range for an equivalent Gaussian beam is of the order of 5 cm. A schematic of the experimental setup used is shown in Fig. 6. Next, we show some profiles experimentally generated for the case of a fourth-order AM beam. We corroborate that the propagation of these beams indeed remains invariant, as is depicted in Fig. 6. Note that the Gaussian envelope must have a considerably large width in order to conserve the nondiffracting behavior of the beam. As an example, if the width is relatively short, there will be a rotation in the intensity profile, as similarly reported for the case of asymmetric Gaussian vortex beams^[26].

Next, we study the behavior of some important physical parameters in the function of the ellipticity and

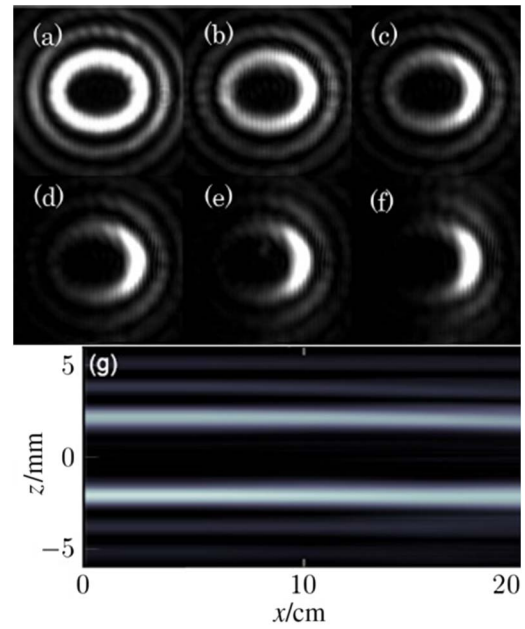


Fig. 6. Experimental fourth-order AM beam obtained with parameters (a) $\alpha = 1$, (b) $\alpha = 1.67$, (c) $\alpha = 5$, (d) $\alpha = 1.14$, (e) $\alpha = 1.19$, and (f) $\alpha = 1.25$. The size of the transverse display area is 5 mm \times 3 mm. (g) Propagation of the AM beam in the x - z plane.

asymmetry. We start by calculating the power or energy flow of the beam, which for a complex scalar optical field is obtained by $P = \int |E|^2 d\vec{r}$ ^[5,22]. We report in Fig. 7 the corresponding behavior of P in the function of the α parameter. Note that for low q values, the function reported indeed shows a minimum value, while for larger q values, the function monotonically decreases. Similarly, for a particular fixed α value, the corresponding q value, where the power achieves its maximum value, can be obtained for either the higher q values, as for the case of $\alpha = 0.1$, or in contrast, the maximum power can be

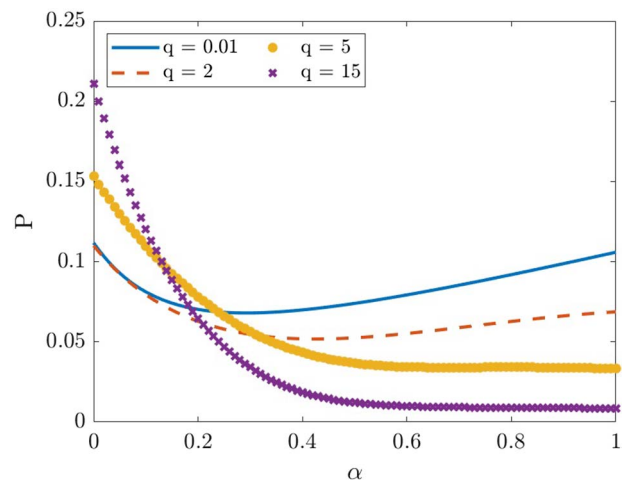


Fig. 7. Power of asymmetric Gaussian–Mathieu beams as a function of the α parameter at different ellipticities given by the q parameter.

obtained for the lower q values, as in the case of $\alpha = 0.5$. Therefore, the overall power distribution in the function of the q and α parameters is in general quite complex, and it must be studied for some particular conditions, as is generally done in previous works, where the applications of the Mathieu functions are studied^[19,20].

We proceed to calculate the OAM projection onto the optical axis, which is defined by $J_z = \text{Im} \int E^*(\vec{r}) \times \nabla E d\vec{r}$. The corresponding values obtained are shown in Fig. 8. Note that similar to the power case, the maximum value of the OAM is a function of the particular combination of q and α parameters. For the case of low q values, the variation of the OAM is lower than for the case of high q values, where the variation can be quite considerable. Note that around $\alpha \approx 0.5$, the OAM is quite similar; thus, it is possible to find AM beams that, in spite of their different transverse structure, can have either similar power or OAM. This fact might be useful in the exploration of the transformation of modes due to the corresponding conservation laws for power and OAM. For $q \rightarrow 0$, we recover the corresponding angular momentum for the scenario of a Bessel–Gauss beam. Note that even for almost $q \approx 0$ and $\alpha = 0$, the corresponding OAM of the AM beams is different from zero; the latter is because we generate AM beams using a superposition of odd and even AM modes. In particular, it is possible to generate AM beams by Eq. (7), where the OAM is indeed zero, by simply taking their pure real or imaginary parts. The function of the OAM reported here is in contrast for the case of asymmetric Laguerre modes^[27], where the corresponding OAM always increases in a quadratic fashion as a function of the asymmetry parameter. Recently, the study of elliptic Gaussian optical vortices^[28] has gained interest due to the ellipticity parameter that can be used for controlling the OAM^[29], and hence, opens up the possibility of being useful in future optical communications systems.

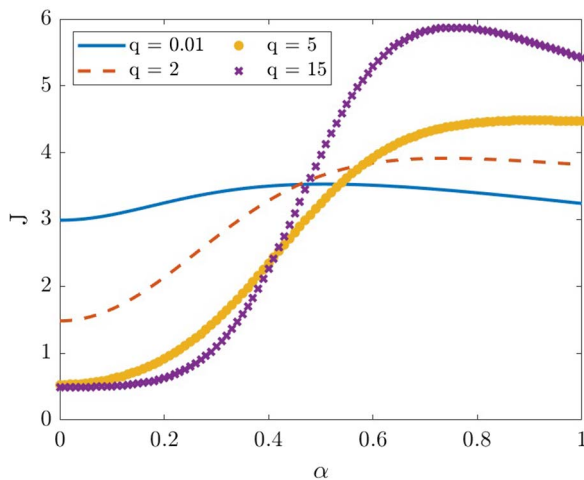


Fig. 8. OAM of asymmetric Gaussian–Mathieu beams as a function of the α parameter at different ellipticities given by the q parameter.

In conclusion, in this Letter, we report the generation of AM beams that can be characterized by three physical parameters: α stands for the degree of asymmetry, β indicates the angular position where the symmetry is broken, and q characterizes the degree of ellipticity. We define these NBs by proposing a simple but very useful angular spectrum. We demonstrate the feasibility of these asymmetric beams with an experimental setup, and we report the corresponding power and OAM for diverse combinations of q and α parameters. We hope that these AM beams can be used in diverse fields, such as micro-manipulation, Bose–Einstein condensates, and soliton routing.

We thank Consejo Nacional de Ciencia y Tecnología (CONACYT) (243284).

References

1. I. Bloch, *Nat. Phys.* **1**, 23 (2005).
2. W. S. Bakr, J. I. Gillen, A. Peng, S. Fölling, and M. Greiner, *Nature* **462**, 74 (2009).
3. K. G. Makris, R. El-Ganainy, D. N. Christodoulides, and Z. H. Musslimani, *Phys. Rev. Lett.* **100**, 103904 (2008).
4. G. K. Brennen, C. M. Caves, P. S. Jessen, and I. H. Deutsch, *Phys. Rev. Lett.* **82**, 1060 (1999).
5. Y. V. Kartashov, V. A. Vysloukh, and L. Torner, *Progr. Opt.* **52**, 63 (2009).
6. Y. V. Kartashov, V. A. Vysloukh, and L. Torner, *Opt. Lett.* **30**, 637 (2005).
7. E. G. Kalnins and W. Miller, Jr., *J. Math. Phys.* **17**, 331 (1976).
8. J. Durnin, J. J. Miceli, Jr., and J. H. Eberly, *Phys. Rev. Lett.* **58**, 1499 (1987).
9. J. Durnin, *J. Opt. Soc. Am. A* **4**, 651 (1987).
10. J. C. Gutiérrez-Vega, M. D. Iturbe-Castillo, and S. Chávez-Cerda, *Opt. Lett.* **25**, 1493 (2000).
11. M. A. Bandres, J. C. Gutiérrez-Vega, and S. Chávez-Cerda, *Opt. Lett.* **29**, 44 (2004).
12. S. López-Aguayo, Y. V. Kartashov, V. A. Vysloukh, and L. Torner, *Phys. Rev. Lett.* **105**, 013902 (2010).
13. V. V. Kotlyar, A. A. Kovalev, and V. A. Soifer, *Opt. Lett.* **39**, 2395 (2014).
14. M. Mazilu, D. J. Stevenson, F. Gunn-Moore, and K. Dholakia, *Laser Photon. Rev.* **4**, 529 (2010).
15. A. A. Kovalev and V. V. Kotlyar, *Opt. Commun.* **338**, 117 (2015).
16. A. A. Kovalev, V. V. Kotlyar, S. G. Zaskanov, and A. P. Porfirev, *J. Opt.* **17**, 035604 (2015).
17. P. A. Sanchez-Serrano, D. Wong-Campos, S. Lopez-Aguayo, and J. C. Gutiérrez-Vega, *Opt. Lett.* **37**, 5040 (2012).
18. S. Orlov and V. Vosylius, in *Conference on Lasers and Electro-Optics Europe and European Quantum Electronics Conference (CLEO/Europe-EQEC)* (IEEE, 2017), paper CM_P_8.
19. U. Felix-Rendon and S. Lopez-Aguayo, *J. Opt.* **20**, 015606 (2017).
20. A. Ruelas, S. Lopez-Aguayo, and J. C. Gutiérrez-Vega, *Opt. Lett.* **33**, 2785 (2008).
21. J. C. Gutiérrez-Vega and M. A. Bandres, *J. Opt. Soc. Am. A* **22**, 289 (2005).
22. V. V. Kotlyar, A. A. Kovalev, R. V. Skidanov, and V. A. Soifer, *J. Opt. Soc. Am. A* **31**, 1977 (2014).
23. C. Lóopez-Mariscal, J. C. Gutiérrez-Vega, G. Milne, and K. Dholakia, *Opt. Express* **14**, 4182 (2006).
24. V. V. Kotlyar, S. S. Stafeev, and A. P. Porfirev, *Opt. Commun.* **357**, 45 (2015).

25. S. Lopez-Aguayo, C. Ruelas-Valdez, B. Perez-Garcia, A. Ortiz-Ambriz, R. I. Hernandez-Aranda, and J. C. Gutiérrez-Vega, *Opt. Lett.* **39**, 6545 (2014).
26. V. V. Kotlyar, A. A. Kovalev, and A. P. Porfirev, *Opt. Lett.* **42**, 139 (2017).
27. A. A. Kovalev, V. V. Kotlyar, and A. P. Porfirev, *Phys. Rev. A* **93**, 063858 (2016).
28. V. V. Kotlyar, A. A. Kovalev, and A. P. Porfirev, *Phys. Rev. A* **95**, 053805 (2017).
29. V. V. Kotlyar and A. A. Kovalev, *Opt. Commun.* **410**, 202 (2018).